Proceedings of the 17th World Congress
The International Federation of Automatic Control
Seoul, Korea, July 6-11, 2008

Real-time Dynamic Optimization of Batch Crystallization Processes

Ali Mesbah[†,‡], Alex N. Kalbasenka[†], Adrie E.M. Huesman[†]
Herman J.M. Kramer[‡] and Paul M.J. Van den Hof[†]

[†] *Delft Center for Systems and Control, Delft University of Technology, Mekelweg 2, 2628 CD Delft, the Netherlands*
[‡] *Process & Energy Laboratory, Delft University of Technology, Leeghwaterstraat 44, 2628 CA Delft, the Netherlands*
(e-mail: ali.mesbah@tudelft.nl)

Abstract: An on-line optimization strategy is developed and applied to a semi-industrial crystallization process. The seeded fed-batch crystallizer is represented by a nonlinear moment model. An optimal control problem pertinent to maximization of the batch crystal yield is solved using the sequential optimization approach. As the dynamic optimizer requires knowledge of the states of the system, an extended Luenberger-type observer is designed to estimate the unmeasured state variable, i.e. solute concentration. Real-time implementations of the proposed strategy reveal the effectiveness of closed-loop optimal control of the crystallizer. The superior performance of the closed-loop implementation to that of the open-loop implementation is attributed to the distinct role of the observer in the feedback control structure that not only accounts for plant-model mismatch by state adaptation, but also enables disturbance handling. Experimental results also demonstrate that the application of the proposed optimal control strategy leads to a substantial increase in the crystal volume fraction at the end of the batch, while the reproducibility of batches with respect to the product crystal size distribution is sustained.

1. INTRODUCTION

A substantial amount of materials in the pharmaceutical, food, and fine chemical processes is produced in crystalline, i.e. solid, form. Batch crystallization is a key separation and purification unit in such industries, with a significant impact on the efficiency and profitability of the overall process. Improved control of such processes offers many possibilities to achieve the stringent requirements of the final product quality, namely crystal size, purity and morphology, and also enhance the process efficiency.

In the face of recent advances in the field of dynamic optimization, the use of optimal operating profiles for the control of batch crystallization processes has awakened the attention in many researchers; see Miller & Rawlings (1994), Lang et al. (1999), Ma et al. (2002), Hu et al. (2005), and Nowee et al. (2007). These studies mostly concerned finding the off-line optimized cooling profiles and their open-loop implementations on batch crystallizers. Nonetheless, the control of batch crystallization processes is a challenging task due to their highly nonlinear behavior, plant-model mismatch, irreproducible start-up, unmeasured process disturbances, and lack of reliable measurements for the system states. It is, therefore, likely that the effectiveness of the off-line optimized profiles degrades in real-time applications.

The performance deterioration of the off-line optimized profiles due to the open-loop implementation motivates the on-line computation of the optimal operating policy during a batch crystallization process. Among the few contributions available in the literature concerning the closed-loop optimal control of batch crystallizers, the work of Chang & Epstein (1987) can be considered as a pioneering study in which the feasibility of a feedback control strategy for batch crystallizers was demonstrated by a number of open-loop and closed-loop simulations. Eaton & Rawlings (1990) proposed a method for optimal feedback control of chemical processes and showed its feasibility on a cooling batch crystallization process. Later, Xie et al. (2001) and Zhang & Rohani (2003) employed an extended Kalman Filter (EKF) in the framework of a feedback optimal control system to account for the plant-model mismatch, and predict the unmeasured state variables. In the latter study, the simulation results revealed that the on-line optimal control strategy would result in substantial improvement of the end product quality in a potash alum batch cooling crystallizer.

Despite the significance of the aforementioned studies, their results were, however, limited to simulation findings; none of them demonstrated the viability of real-time dynamic optimization of batch crystallization processes experimentally. This study concerns the design and real-time implementation of an on-line optimization strategy for seeded fed-batch evaporative crystallization of an ammonium sulphate-water system. Unlike batch cooling crystallization processes, the optimal control of batch evaporative crystallization has gained little attention in the literature. The optimal control problem presented in this paper is solved using the sequential optimization approach. The performance of the proposed control strategy is examined experimentally by a number of open-loop and closed-loop

implementations on a semi-industrial 75-liter draft tube crystallizer.

This paper is comprised of five sections. In the following section, the model of the seeded fed-batch evaporative crystallizer is presented. Section 3 discusses the formulation of the optimal control problem, as well as the design of an extended Luenberger-type observer. The experimental results of batch crystallization optimization are presented in section 4, while conclusions and future research directions are given in section 5.

2. CRYSTALLIZATION MODEL

The mathematical models of solution crystallization processes are typically obtained through the application of a population balance equation, mass balance equations for solvent and solute, energy balance equation, and expressions describing the variation of the equilibrium concentration. The population balance equation accounts for the evolution of crystal particles along temporal and size domains. Under the assumptions of mixed suspension, constant crystallizer volume, nucleation of crystals of infinitesimal size, and negligible breakage and agglomeration, the dynamic population balance equation for a semi-batch crystallization process simplifies to (Randolph & Larson, 1988):

$$V\frac{\partial n(L,t)}{\partial t} + V\frac{\partial (n(L,t)G)}{\partial L} = VB(L,t) - Q_p n(L,t) \quad (1)$$

where n is the number density ($\# \cdot m^{-3} \cdot m^{-1}$), G is the growth rate ($m \cdot s^{-1}$), B is the nucleation rate ($\# \cdot m^{-3} \cdot m^{-1} \cdot s^{-1}$), L is the characteristic crystal size (m), V is the crystallizer volume (m^3), and Q_p is the sample stream flow rate ($m^3 \cdot s^{-1}$).

Numerical solution of the population balance equation often requires considerable computational effort that might render the real-time implementation of model based control strategies infeasible. The method of moments is, therefore, applied to equation (1) in order to convert the population balance equation into a set of computationally affordable Ordinary Differential Equations (ODEs). With defining the i^{th} moment of $n(L,t)$ as:

$$m_i = \int_0^\infty L^i n(L,t)\, dL \quad i = 0, \ldots, 4 \quad (2)$$

multiplying equation (1) by $L^i dL$ and, subsequently, integrating over the entire crystal size domain result in the following set of ODEs that describes the evolution of moments of the Crystal Size Distribution (CSD) in time:

$$\begin{aligned} \frac{dm_0}{dt} &= B_0 - \frac{m_0 Q_p}{V} \\ \frac{dm_i}{dt} &= iGm_{i-1} - \frac{m_i Q_p}{V} \quad i = 1, \ldots, 4. \end{aligned} \quad (3)$$

Here B_0 represents the total rate of nucleation ($\# \cdot m^{-3} \cdot s^{-1}$).

Among various types of nucleation mechanism, this work only considers the particle formation from crystal surfaces, i.e. secondary nucleation, since it is the dominant nucleation mechanism occurring in seeded batch crystallizers. The empirical expressions realized for the total nucleation rate, and the size independent crystal growth rate are as follows:

$$B_0 = k_b m_3 G \quad (4)$$

$$G = k_g (C - C^*)^g \quad (5)$$

The nucleation rate constant k_b, the growth rate constant k_g, and the growth rate exponent g are the kinetic parameters corresponding to the ammonium sulphate-water system. Furthermore C and C^* are the solute concentration and the equilibrium concentration, respectively; their difference determines the driving force of the crystallization process, known as the supersaturation.

Table 1. Model parameters

Symbol	Value	Unit
C^*	0.46	$kg_{solute}/kg_{solution}$
g	1.0	-
H_c	60.75	kJ/kg
H_L	69.86	kJ/kg
H_v	2.59×10^3	kJ/kg
K_v	0.43	-
k_b	1.02×10^{14}	$\#/m^4$
k_g	7.50×10^{-5}	m/s
Q_p	1.73×10^{-6}	m^3/s
V	7.50×10^{-2}	m^3
ρ_c	1767.35	kg/m^3
ρ_L	1248.93	kg/m^3

In the face of isothermal operation of the evaporative crystallizer, a single expression is derived for the solute concentration using the mass and energy balance equations:

$$\frac{dC}{dt} = \frac{\frac{Q_p(C^*-C)}{V} + 3K_v G m_2 (k_1 + C)}{1 - K_v m_3} + \frac{k_2 H_{in}}{1 - K_v m_3} \quad (6)$$

with constant coefficients given by:

$$k_1 = \frac{H_v C^*}{H_v - H_L}\left(\frac{\rho_c}{\rho_L} - 1 + \frac{\rho_L H_L - \rho_c H_c}{\rho_L H_v}\right) - \frac{\rho_c}{\rho_L} \quad (7)$$

$$k_2 = \frac{C^*}{V \rho_L (H_v - H_L)} \quad (8)$$

where K_v is the crystal volumetric shape factor, H_{in} is the heat input to the crystallizer (kW), ρ_L is the saturated solution density ($kg \cdot m^{-3}$), and ρ_c is the density of crystals ($kg \cdot m^{-3}$). H_L, H_c and H_v are the solution, crystals and vapor specific enthalpies ($kJ \cdot kg^{-1}$), respectively. The physical properties of the ammonium sulphate-water system, as well as the nucleation and growth rate kinetic parameters are listed in Table 1.

From the aforementioned analysis, it follows that the dynamic behavior of the system under investigation is governed by a set of Differential Algebraic Equations (DAEs), equations (3-8). Hence, the five leading moments of the CSD, and the solute concentration are the state variables determining the dynamics of the system. Actual measurements are only available for the moments of the CSD.

In the batch experiments, large seed loads are used that result in relatively low supersaturation levels (Doki et al., 2002). Under these conditions, the effect of secondary nucleation is minimized and, consequently, the crystal growth mainly dictates the dynamics of the crystal size distribution throughout the batch. Hence, the CSD in

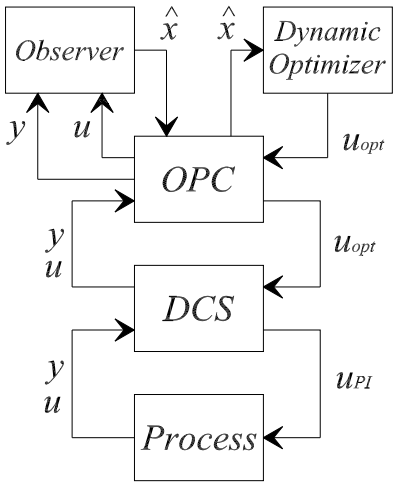

Fig. 1. Block diagram of the control system

such process is unimodal and, therefore, can be reasonably represented by the mean crystal size and the CSD width using the moment model. The nonlinear moment model was experimentally verified to be an adequate description of the process at hand (Mesbah et al., 2007).

3. ON-LINE OPTIMAL CONTROL STRATEGY

3.1 Dynamic Optimization

The effective strategy to be realized for optimal control of crystallization processes mainly depends on the product specifications, as well as the properties of the crystallization system under investigation. Achievement of the desired final product characteristics is often of higher importance than maximization of process yield or energy saving considerations. A preceding study on the controllability analysis of the 75-liter draft tube crystallizer conducted by Kalbasenka et al. (2007) revealed that the initial conditions have a profound impact on the fed-batch process. It has been shown that a good reproducibility of batches with respect to the crystal size can only be obtained by means of a proper seeding strategy.

In this study, the primary goal is to maximize the batch crystal yield while the reproducibility of batch runs, as well as the fulfilment of the desired product specifications is sustained. This objective is achieved by manipulation of the supersaturation profile. In an evaporative crystallizer, the supersaturation trajectory is dependent on the heat input to the crystallizer. Hence, the heat input can be utilized as a manipulated variable to control the non-equilibrium driving force of the process and, consequently, optimize the batch crystal yield. As most of the crystallization phenomena are supersaturation-dependent, variations in the heat input should be constrained in such a way as to avoid degradation of the product quality caused by e.g. irregular crystal growth, impurity uptake, solvent inclusion etc.

An optimal control problem is thereby formulated to determine the heat input profile that maximizes an objective function pertinent to the batch crystal yield while certain constraints are imposed on the heat input and crystal growth rate to avoid degradation of the product quality. The optimal control problem is expressed as follows:

$$\begin{aligned} \min_{H_{in}(t)} \quad & \frac{\int_0^{t_f} (100\frac{G(t)-G_{max}}{G_{max}})^2\, dt}{\int_0^{t_f} dt} \\ \text{s.t.} \quad & \text{equations (3)-(8)} \\ & G(t) \leqslant G_{max} = 2.5 \times 10^{-8} \quad m/s \\ & 9 \leqslant H_{in}(t) \leqslant 13 \quad kW \end{aligned} \tag{9}$$

where H_{in} is the vector of the piecewise constant heat input profile, and G_{max} is the maximum crystal growth rate. The lower bound of heat input is kept at a relatively high value to ensure survival of ground seeds in the crystallizer during the initial phase of the process, whereas an approximation of the upper actuator constraint is taken as the upper heat input bound. An inequality constraint is also imposed on the crystal growth rate to avoid the formation of irregularly shaped crystals. The optimal control problem described in (9) is, therefore, equivalent to maximization of the batch crystal yield while sustaining the product quality.

Among several methods for computing solution to the multivariable optimization problem, the sequential approach proposed by Biegler & Cuthrell (1985) is employed to solve the optimization problem (9). In this approach, the optimal control problem is transformed into a Nonlinear Programming Problem (NLP) by parameterization of the control input variable. An ODE solver is, thereby, used in combination with an optimization algorithm to solve the NLP problem sequentially. The major advantage of the sequential approach is the reduced dimensionality of the nonlinear program since the number of parameters in the control parametrization problem remains small. In this study, the set of differential-algebraic equations (3-8) is integrated using the Euler method, while the MATLAB optimization function, i.e. fmincon, is utilized to solve the NLP problem in which the heat input is parameterized.

3.2 Observer Design

Real-time implementation of the dynamic optimizer requires knowledge of the current states of the system. As actual measurements are not available for the solute concentration, an observer based on nonlinear extension of the Luenberger state estimation technique (Ciccarella et al., 1993) is used to estimate the evolution of supersaturation during the fed-batch crystallization process. For the system under investigation, the performance of the extended Luenberger-type observer appeared to be superior to that of an extended Kalman filter (Kalbasenka et al., 2006).

In order to design the observer, the moment model described by equations (3-8) is reformulated in the following form:

$$\frac{dx(t)}{dt} = f(x(t)) + g(x(t))u(t) \quad x(0) = x_0 \tag{10}$$

$$y(t) = h(x(t)) \tag{11}$$

where the state vector $x(t) \in \Re^{n_x}$, the output vector $y(t) \in \Re^{n_y}$, and the input vector $u(t) \in \Re^{n_u}$ are defined as:

$$x(t) = [m_0 \quad m_1 \quad m_2 \quad m_3 \quad m_4 \quad C]^T \tag{12}$$

Table 2. Scaling factors and optimization parameters in equation (19)

Index	1	2	3	4	5
a_i	1×10^{-10}	1×10^{-6}	1×10^{-2}	1×10^{2}	1×10^{5}
K_i	2.72×10^{-3}	84.5	0.117	0.441	0.464

$$y(t) = [m_0 \quad m_1 \quad m_2 \quad m_3 \quad m_4]^T \tag{13}$$

$$u(t) = H_{in}. \tag{14}$$

The observer equation is expressed as:

$$\frac{d\widehat{x}(t)}{dt} = f(\widehat{x}(t)) + g(\widehat{x}(t))u(t) + [Q(\widehat{x}(t))]^{-1} K E(t) \tag{15}$$

where $\widehat{x}(t)$ is the estimated state vector, $Q(\widehat{x}(t))$ is the observability matrix, K is the finite gain vector of the observer to be determined by tuning, and $E(t)$ denotes the difference between the measured and estimated outputs, i.e. error signal:

$$E(t) = y(t) - h(\widehat{x}(t)). \tag{16}$$

As tuning is a rather tedious task to determine the gain vector K, a slightly different formulation of equation (15) is used:

$$\frac{d\widehat{x}(t)}{dt} = f(\widehat{x}(t)) + g(\widehat{x}(t))u(t) + \widehat{K} E(t) \quad \widehat{x}(0) = \overline{x} \tag{17}$$

in which $\widehat{K} \in \Re^{n_x \times n_y}$ is a constant matrix:

$$\widehat{K} = \begin{bmatrix} 0 & 0 & 0 & K_1 & 0 \\ 0 & 0 & 0 & 0 & K_2 \\ 0 & 0 & K_3 & 0 & 0 \\ 0 & 0 & 0 & K_4 & 0 \\ 0 & 0 & 0 & 0 & K_5 \\ 0 & 0 & 0 & 0 & 0 \end{bmatrix}. \tag{18}$$

It is self-evident that entries of the last row in matrix (18) are zero since the error signal for the sixth state, i.e. solute concentration, is not available. Due to the absence of accurate measurements for m_0 and m_1, these two state variables are estimated using error signals defined on the basis of m_3 and m_4 measurements, respectively.

The matrix $\widehat{K}$ is then determined as a solution to the following optimization problem formulated in gPROMS (PSE Ltd., UK):

$$\min_{K_i} \quad \sum_{i=1}^{5} a_i \frac{\int_0^{t_f} |x_i(t) - \widehat{x}_i(t)|\, dt}{\int_0^{t_f} dt} \tag{19}$$

$$\text{s.t.} \quad \text{equation (17).}$$

Numerical values of the scaling constants a_i, and the entries of matrix $\widehat{K}$ are given in Table 2. The scaling constants account for the greatly differing order of magnitude of the states.

4. RESULTS AND DISCUSSION

The effectiveness of the proposed control strategy is evaluated experimentally for fed-batch evaporative crystallization of an ammonium sulphate-water system. The optimal control strategy is implemented on a 75-liter draft tube crystallizer in both open-loop, i.e. without observer and state feedback, and closed-loop modes. The crystallizer is equipped with an on-line laser diffraction instrument

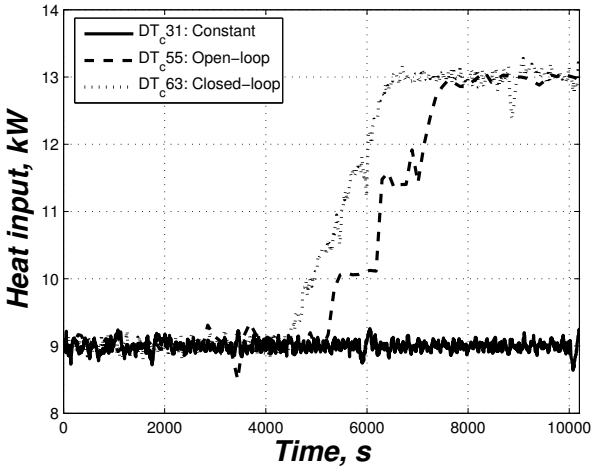

Fig. 2. Heat input profiles

(HELOS-Vario, Sympatec, Germany) to measure evolution of the product CSD during the batch. The predetermined supersaturation level at which the ground seeds are inserted into the crystallizer is measured using an in-line concentration measuring probe (LiquiSonic 20, SensoTech, Germany).

The feedback control scheme used to compute and implement the optimal heat input profile on the crystallizer is depicted in Fig. 1. A Distributed Control System (DCS, CENTUM CS3000, Yokogawa, Japan) forms the basic control layer consisting of Proportional Integral (PI) loops, as well as extensions to control process variables such as levels, temperatures, pressures, heat input etc. The heat input to the crystallizer is optimized using the nonlinear moment model in the Dynamic Optimizer where input constraints are incorporated into the optimal control problem that is solved on-line. In order to determine the current states of the system, an observer is designed to estimate the unmeasured state variable, i.e. solute concentration. The observer also accounts for the process-model mismatch. Therefore, the feedback control structure effectively handles the uncertainties that are associated with the model's parameters.

The core component of this multi-layer control architecture is an OPC (**O**LE (Object Linking and Embedding) for **P**rocess **C**ontrol) server (IPCOS, the Netherlands) that facilitates the communication among various modules in the control system. The process measurements y collected by the DCS are passed to the observer via the OPC server. The OPC also sends the optimal heat input profile u_{opt} computed on the basis of the estimated states $\widehat{x}$ to the lower level PI controller that keeps the heat input as close to the optimal set points as possible by manipulating the available actuators of the process within certain bounds.

As product quality is strongly dependent on the growth rate profile throughout the batch, the variation of crystal growth rate in relation to three different heat input profiles is examined. The heat input and crystal growth rate profiles are depicted in Fig. 2 and Fig. 3, respectively. The undesirable effects of secondary nucleation, as well as excessive growth rates can be minimized by imposing a maximum growth rate constraint in the course of the

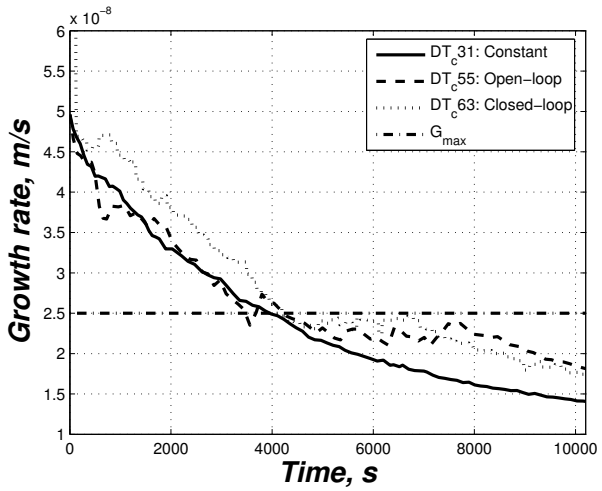

Fig. 3. Crystal growth rate profiles

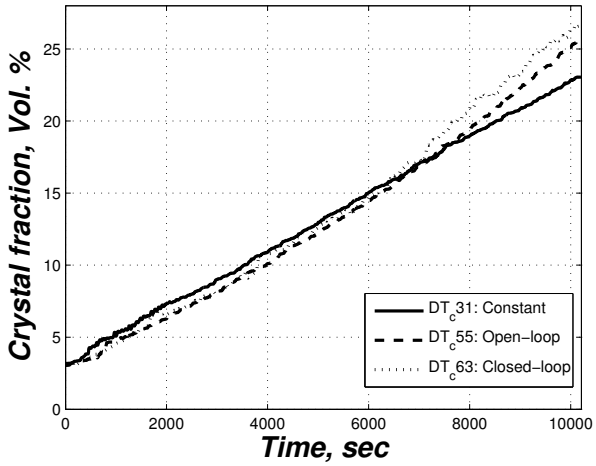

Fig. 4. Comparison of the crystal fractions

batch process. As can be seen, when the heat input is kept constant at $9kW$ during experiment DT_c31, the growth rate steadily drops without following the maximum growth rate shown by the dashed-dotted line in Fig. 3. This behavior suggests that an effective control strategy is required to meet the growth rate constraint. An off-line dynamic optimization is, therefore, performed and implemented in open-loop mode during experiment DT_c55, where the heat input is manipulated manually. Fig. 3 shows that the growth rate yet again fails to follow the constraint at the optimal heat-input profile implemented in the open-loop mode.

In order to force the process to follow the constraint more closely, the optimal control strategy is implemented in closed-loop mode throughout experiment DT_c63. As demonstrated in Fig. 3, once the growth rate crosses the constraint at $t = 4200s$, it is forced to follow the maximum growth rate by raising the heat input to the crystallizer. However, the constraint can no longer be tracked when the heat input reaches its upper bound of $13kW$ at $t = 6900s$ as shown in Fig. 2. Consequently, the growth rate gradually decreases while the heat input remains at its maximum admissible value. It is evident that in spite of the fact that the constraint is not met in the initial phase of the batch until the growth rate hits the maximum growth rate, no control action is taken since the heat input is constrained by a lower bound, i.e. $9kW$. The lower heat input bound ensures the survival of ground seeds by keeping the supersaturation at somewhat high levels. It is worth noting that the differences in the initial growth rate profiles of various batches are due to uncertain initial conditions at the seeding point.

Fig. 3 in fact exhibits the effectiveness of closed-loop optimal control of the crystallizer, where better constraint tracking is achieved till actuation limitations render the optimal control of the batch process impossible. The improvement in the performance of the optimal controller can be attributed to the feedback structure, as well as the receding horizon implementation of the control system. In such control framework, the observer not only accounts for the plant-model mismatch but also enables effective disturbance handling.

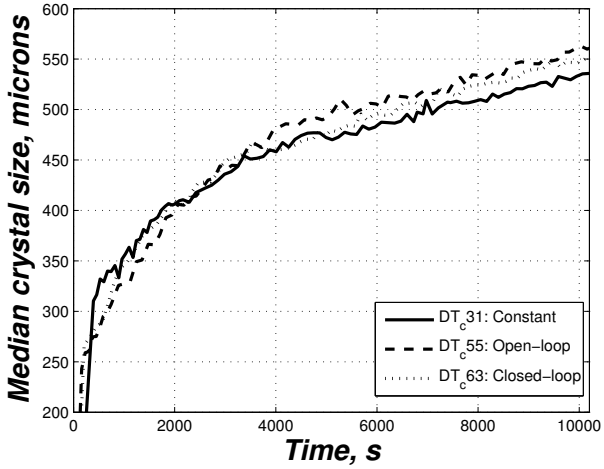

Fig. 5. Comparison of the median crystal size

The volume fractions of crystals measured in the course of various batches are depicted in Fig. 4. The crystal fractions at the batch end of experiments DT_c55 and DT_c63, during which optimal control is implemented, are $26vol.\%$ and $27vol.\%$ respectively, whereas in the experiment of constant heat input profile the crystal fraction is $23vol.\%$. Therefore, the implementation of the optimal control strategy in either mode leads to a substantial increase of almost 15% in the crystal volume fraction at the end of the batch.

As can be inferred from Fig. 5, the heat input does not have a significant impact on the median crystal size. This shows that the supersaturation level is manipulated by the heat input in such a way that the secondary nucleation does not increase considerably throughout the batch and, therefore, does not have a pronounced effect on the product crystal size distribution. This is due to the effective control of the secondary nucleation achieved by means of the proper seeding strategy.

5. CONCLUSIONS AND FUTURE WORK

This study concerns the optimal operation of a semi-industrial batch crystallization process. It shows that dy-

namic optimization in combination with a nonlinear process model provides an effective and efficient approach to solve real-time optimal control problems in batch crystallization processes.

An on-line strategy is proposed for optimal control of a seeded fed-batch evaporative crystallizer. An extended Luenberger-type observer is employed to provide estimations for the unmeasured state variable, which makes the real-time implementation of the feedback control structure possible. The closed-loop implementation of the optimal control strategy displays a superior performance in comparison with the open-loop implementation. This demonstrates the role of the observer in the feedback control structure that accounts for the deviation of model from the process, and also enables a better disturbance handling.

In future, real-time solution to the optimal control problem discussed in this study will be investigated using the simultaneous dynamic optimization approach. This approach, which is expected to be computationally more efficient, enables the direct application of population balance equation as the underlying process model.

ACKNOWLEDGEMENTS

The authors would like to express their sincerest gratitude to J. Landlust for his assistance in implementing the control strategy. The financial support of SenterNovem, BASF, and BP is also gratefully acknowledged.

REFERENCES

L.T. Biegler, and J.E. Cuthrell. Improved infeasible path optimization for sequential modular simulators-II: The optimization algorithm. *Comp. Chem. Eng.*, 9:257–267, 1985.

C.T. Chang, and M.A.F. Epstein. Simulation studies of a feedback control strategy for batch crystallizers. In *Fundamental Aspects of Crystallization Precipitation Processes*, pages 110–119. AICHE, New York, 1987.

G. Ciccarella, M. Dalla Mora, and A. Germani. A Luenberger-like observer for nonlinear systems. *Int. J. Control*, 57:537–556, 1993.

N. Doki, N. Kubota, M. Yokota, and A. Chianese. Determination of critical seed loading ratio for the production of crystals of uni-modal size distribution in batch cooling crystallization of potassium alum. *J. Chem. Eng. Japan*, 35:670–676, 2002.

J.W. Eaton, and J.B. Rawlings. Feedback control of chemical processes using on-line optimization techniques. *J. Computers Chem. Eng.*, 14:469–479, 1990.

Q. Hu, S. Rohani, D.X. Wang, and A. Jutan. Optimal control of a batch cooling seeded crystallizer. *Powder Technology*, 156:170–176, 2005.

A.N. Kalbasenka, L. Spierings, A.E.M. Huesman, and H.J.M. Kramer. Application of seeding as a process actuator in a model predictive control framework for fed-batch crystallization of ammonium sulphate. *Part. Part. Syst. Charact.*, 24:140–48, 2007.

A.N. Kalbasenka, J. Landlust, A.E.M. Huesman, and H.J.M. Kramer. Application of observation techniques in a model predictive control framework of fed-batch crystallization of ammonium sulphate. In *Proceedings of* 5^{th} *World Congress on Particle Technology*. Orlando, 2006.

Y.D. Lang, A.M. Cervantes, and L.T. Biegler. Dynamic optimization of a batch cooling crystallization process. *Ind. Eng. Chem. Res.*, 38:1469–1477, 1999.

D.L. Ma, D.K. Tafti, and R.D. Braatz. Optimal control and simulation of multidimensional crystallization process. *Computers Chem. Eng.*, 26:1103–1116, 2002.

A. Mesbah, A.N. Kalbasenka, A.E.M. Huesman, H.J.M. Kramer, P.J. Jansens, and P.M.J. Van den Hof. Real-time dynamic optimization of crystal yield in a fed-batch evaporative crystallization of ammonium sulphate. In *Proceedings of the* 14^{th} *International Workshop on Industrial Crystallization*, pages 81–88. Cape Town, 2007.

S.M. Miller, and J.B. Rawlings. Model identification and control strategies for batch cooling crystallizers. *AIChE*, 40:1312–1327, 1994.

S.M. Nowee, A. Abbas, and J.A. Romagnoli. Optimization in seeded cooling crystallization: A parameter estimation and dynamic optimization study. *Chem. Eng. Process.*, 46:1096–1106, 2007.

A. Randolph, and M.A. Larson. *Theory of Particulate Process*. Academic Press, San Diego, 1988.

W. Xie, S. Rohani, and A. Phoenix. Extended Kalman filter based nonlinear geometric control of a seeded batch cooling crystallizer. *Chem. Eng. Comm.*, 187: 229–249, 2001.

G.P. Zhang, and S. Rohani. On-line optimal control of a seeded batch cooling crystallizer. *Chem. Eng. Sci.*, 58:1887–1896, 2003.